Phase Structure of Poly(3-hydroxy butyrate)/Poly(vinyl acetate) Blends Probed by Small-Angle X-ray Scattering

Hsiu-Jung Chiu,[†,⊥] Hsin-Lung Chen,[*,†] Tsang-Lang Lin,[‡] and J. S. Lin[§]

Department of Chemical Engineering, National Tsing Hua University, Hsin-Chu, Taiwan 30013, R. O. C.; Department of Engineering and System Science, National Tsing Hua University, Hsin-Chu, Taiwan 30013, R. O. C.; and Solid State Division, Oak Ridge National Laboratory, Oak Ridge, Tennessee 37831

Received March 1, 1999; Revised Manuscript Received May 18, 1999

ABSTRACT: The semicrystalline morphology of poly(3-hydroxy butyrate) (PHB)/poly(vinyl acetate) (PVAc) blends at four crystallization temperatures (T_c = 70, 90, 110, and 125 °C) was probed by small-angle X-ray scattering (SAXS). Morphological parameters including the crystal thickness (l_c) and the amorphous layer thickness (l_a) were deduced from the interphase distribution function. Blending with PVAc thickened the PHB crystals. The amorphous layers were also swollen upon blending, but l_a displayed a maximum in its variation with PVAc composition. A zero-angle scattering was observed in the Lorentz-corrected SAXS profiles of PHB/PVAc 60/40 blend crystallized at 110 and 125 °C and 50/50 composition crystallized at 90−125 °C. Such a zero-angle scattering was attributed to the presences of amorphous domains between the lamellar stacks so as to generate gaps in the sequential stacking of lamellae. These amorphous domains were generated by the interfibrillar segregation of PVAc, where PVAc was expelled beyond several layers of lamellae and subsequently resided in the regions between the lamellar stacks. On the basis of the composition variation of l_a, the observation of zero-angle scattering, and the magnitude of the volume fraction of lamellar stacks, it was concluded that when PVAc composition was ≤20 wt %, the morphology was predominantly characterized by the interlamellar segregation; above this composition, interlamellar and interfibrillar segregation coexisted, and the extent of interfibrillar segregation increased with the increases of PVAc composition and crystallization temperature.

Introduction

Bacterially synthesized poly(3-hydroxy butyrate) (PHB) is a crystalline biodegradable polymer with a melting point of ca. 180 °C. PHB formed miscible blends with various commercial polymers such as poly(ethylene oxide) (PEO),[1−4] poly(vinylidene fluoride) (PVDF),[5,6] poly(vinyl chloride) (PVC),[7,8] poly(epichlorohydrin),[9,10] poly(4-vinylphenol) (PVPh),[11] and poly(vinyl acetate) (PVAc).[12,13] The system of interest here is the blend of PHB and PVAc. PHB/PVAc is a crystalline/amorphous system for which the crystallization usually involves two types of polymer transport: diffusion of the crystalline component toward the crystal growth front and simultaneous segregation of the amorphous diluent away from the growth front. The diluent segregation can take place on three length scales, namely, interlamellar, interfibrillar, and interspherulitic.[14−16] Interlamellar segregation occurs when the diluent is incorporated into the amorphous regions between individual lamellae. Interfibrillar segregation is characterized by the segregation of the amorphous diluent to the regions between the lamellar stacks, which consequently generates amorphous domains in between the lamellar stacks. Interspherulitic segregation is associated with the longest segregation distance, where the diluent is expelled out of the spherulites. Different morphological patterns may coexist in a given blend, leading to multiple locations for the amorphous diluent.[17−19]

Small-angle X-ray scattering (SAXS) is a very powerful tool for probing the detailed microstructure of crystalline/amorphous blends. The morphological parameters in the lamellar level such as the long period (L), crystal thickness (l_c), and amorphous layer thickness (l_a) can be deduced via quantitative analysis of the SAXS profiles. Close examination on the composition variation of l_a may reveal the existence of interlamellar segregation.[20−22] The volume fraction of lamellar stacks (ϕ_s) given by the ratio of bulk crystallinity (ϕ_c) to linear crystallinity (ϕ_c^{lin}) could serve as a measure for the extent of interlamellar segregation.[17−19]

In the present study, we utilize SAXS to probe the morphological structure of PHB/PVAc blends at various crystallization temperatures (T_c). One objective of this study is to demonstrate the presence of "zero-angle scattering" in the SAXS profiles of semicrystalline PHB/PVAc and address its implication on the morphological structure. The effects of composition and temperature on the morphological pattern of PHB/PVAc will also be critically discussed.

Experimental Section

Materials and Sample Preparation. PHB with $M_n = 2.93 \times 10^5$ and $M_w = 6.5 \times 10^5$ and PVAc with M_w = 83 000 were purchased from Aldrich Chemical Co. PHB was blended with PVAc by solution casting using DMF as the cosolvent. Specimens for SAXS study were prepared by pressing the blends between two pieces of Teflon films on a Linkam HFS91 hot stage at 190 ± 0.2 °C for 1 min, followed by quickly transferring the samples into an oven equilibrated at the desired crystallization temperatures (T_c = 70, 90, 110, and 125 °C). Since the SAXS analysis presented here requires the spherulites within the sample to be volume filling, crystallizations

* To whom correspondence should be addressed.
† Department of Chemical Engineering, National Tsing Hua University.
‡ Department of Engineering and System Science, National Tsing Hua University.
§ Solid State Division, Oak Ridge National Laboratory.
⊥ Current address: Department of Chemical Engineering, Tahwa Institute of Technology, Chung-Lin, Hsin-Chu, Taiwan 30740, R. O. C.

10.1021/ma990304+ CCC: $18.00
Published on Web 07/09/1999

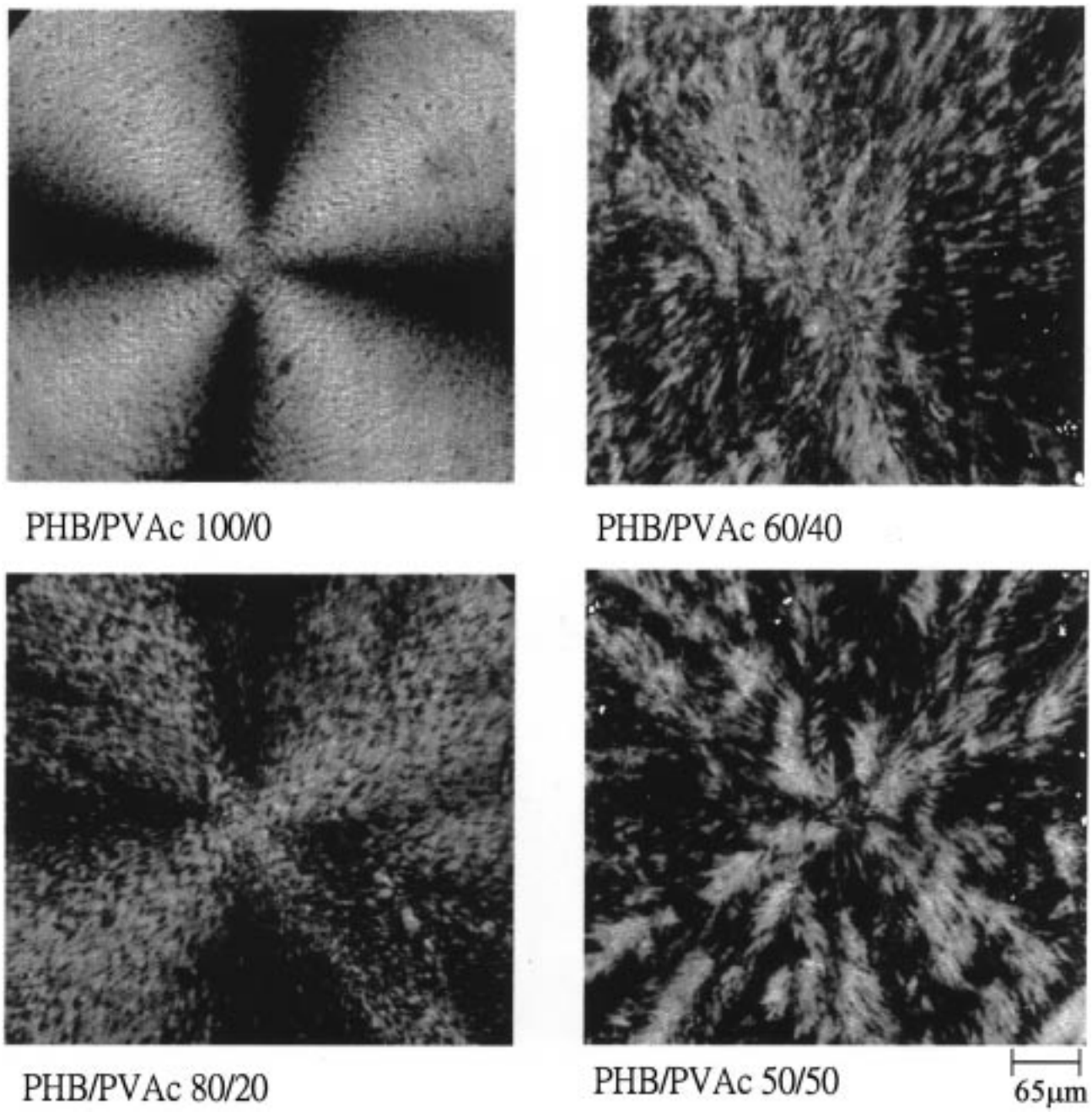

Figure 1. A series of optical micrographs showing the variation in spherulitic morphology with PVAc composition for PHB/PVAc blends crystallized at 90 °C.

were conducted for 72 h. Optical microscopy confirmed that volume-filling spherulites were obtained through such a crystallization condition.

Bulk Crystallinity Measurements. Bulk crystallinities of semicrystalline PHB/PVAc blends were calculated from the enthalpy of melting (Δh_f). The samples used for Δh_f measurements were cut directly from the specimens for SAXS measurement. The enthalpy of melting was measured by a TA Instrument 2000 differential scanning calorimeter (DSC). The bulk crystallinity was calculated by taking 146 J/g as the enthalpy of melting of 100% crystalline PHB.[23]

SAXS Measurement. SAXS measurements were conducted on the SAXS instruments at either National Tsing Hua University (NTHU) or Oak Ridge National Laboratory (ORNL). The SAXS setup at NTHU has been described in our previous publications.[18,19] The ORNL 10 m SAXS instrument has a sample-to-detector distance of 3.119 m using Cu Kα radiation (λ = 1.54 Å) and a 20 × 20 cm^2 two-dimensional position-sensitive detector with each virtual cell element of about 3 mm apart. The scattering intensity was stored in a 64 × 64 data array. Corrections were made for instrumental backgrounds, dark current due to cosmic radiation and electronic noises, and detector nonuniformity and efficiency (via an Fe^{55} radioactive standard which emits γ-rays isotropically) on a cell-by-cell basis. The data were radially (azimuthually) averaged in the q range: 0.16 nm^{-1} < q < 1.6 nm^{-1} ($q = 4\pi/\lambda \sin(\theta/2)$, where λ is the X-ray wavelength and θ is the scattering angle).

Results and Discussion

Figure 1 shows the spherulitic morphology of PHB and PHB/PVAc blends crystallized at 90 °C. The spherulites of neat PHB display smooth texture and clear Maltese cross pattern. Coarsening of spherulitic texture and disruption of Maltese cross pattern occurred upon blending with PVAc. Since volume-filling spherulites were observed, the changes of spherulitic texture basically indicate the intraspherulitic segregation of PVAc.

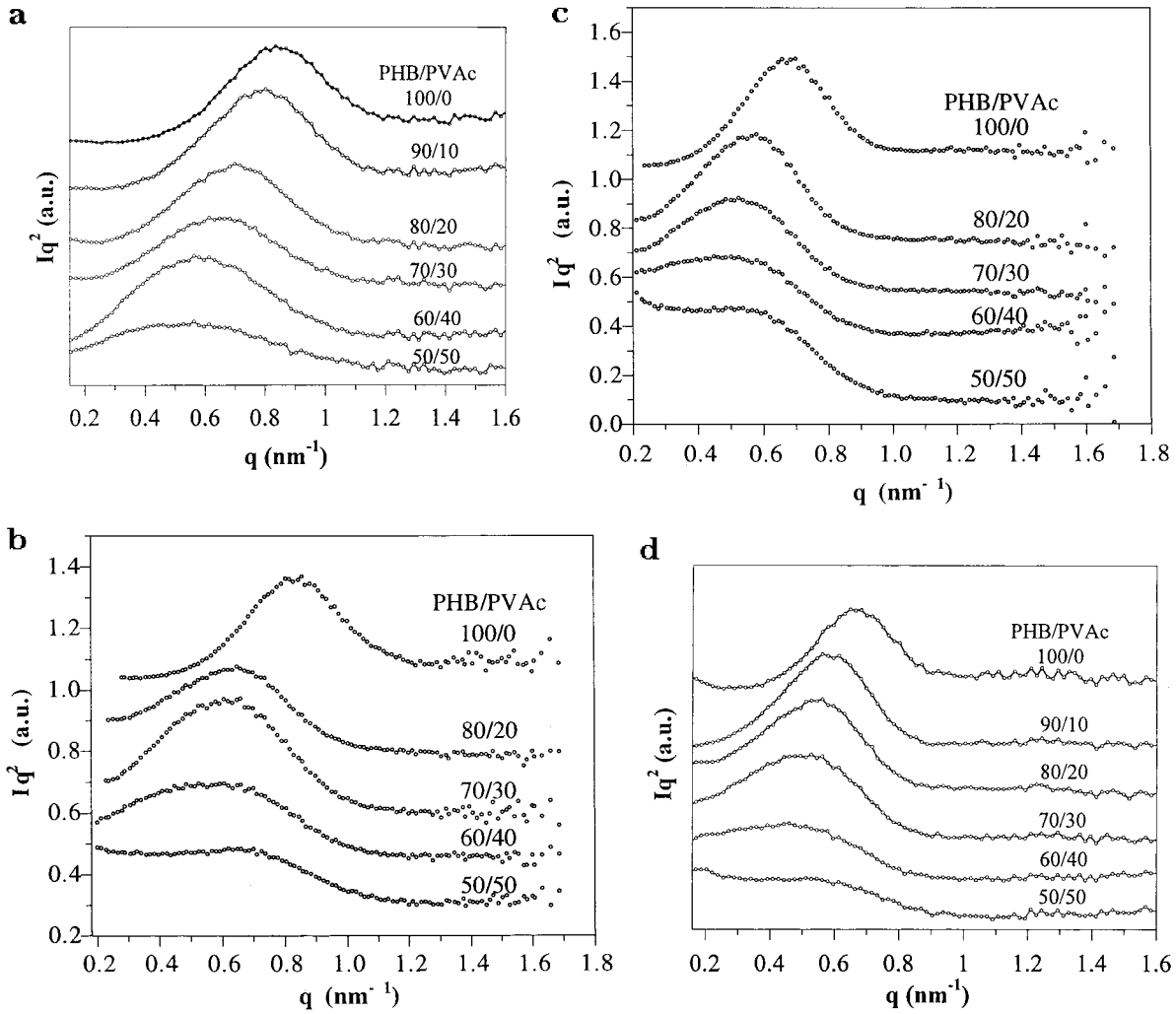

Figure 2. Profiles of Lorentz-corrected intensity of PHB/PVAc blends crystallized at (a) 70, (b) 90, (c) 110, and (d) 125 °C. The compositions are indicated in the figures.

Figure 2 displays the profiles of Lorentz-corrected intensity of PHB/PVAc crystallized at a series of T_c's. At a given T_c, the scattering peak shifts toward lower angle with increasing PVAc composition, indicating that the weight-average long period calculated from the Bragg's law increases. The crystal thickness (l_c) and amorphous layer thickness (l_a) associated with the lamellar stacks were determined from the interphase distribution function, $g_1(z)$, defined as the second derivative of the one-dimensional correlation function, $\gamma(z)$:[24−26]

$$g_1(z) = \gamma''(z) \tag{1}$$

where $\gamma(z)$ is given by[27]

$$\gamma(z) = \frac{1}{Q}\int_0^\infty I(q)q^2 \cos(qz)\, dq \tag{2}$$

where z is the direction along which the electron density is measured and Q is the scattering invariant.

Figure 3 presents the interphase distribution functions of PHB/PVAc crystallized at 70 °C. The first minimum of $g_1(z)$ provides the number-average value of long period, and the first maximum yields the average thickness of the thinner layers (l_1) in the lamellar stacks.[25] The thickness of the thicker layer is given by $l_2 = L - l_1$. On the basis of the Babinet's reciprocity theorem,[28] it is not possible to distinguish directly

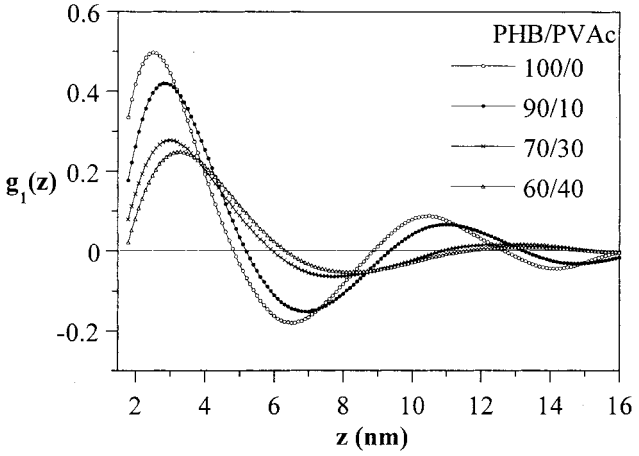

Figure 3. Interphase distribution functions of PHB/PVAc blends crystallized at 70 °C. The compositions are indicated in the figure.

whether l_1 corresponds to l_c or l_a. The assignment of l_1 and l_2 is governed by the magnitude of the linear crystallinity, ϕ_c^{lin}, defined as

$$\phi_c^{lin} = \frac{l_c}{L} = \frac{l_c}{l_c + l_a} \tag{3}$$

When the linear crystallinity is lower than 0.5, the

crystals contribute to the smaller thickness; thus $l_1 = l_c$ and $l_2 = l_a$. The inverse is true for $\phi_c^{lin} > 0.5$. Provided that the spherulites in the sample are volume-filling, the linear crystallinity is related to the bulk crystallinity, ϕ_c, by

$$\phi_c = \phi_s \phi_c^{lin} \tag{4}$$

where ϕ_s is the volume fraction of lamellar stacks. Since $\phi_s \leq 1$, eq 4 prescribes that the bulk crystallinity cannot be higher than the linear crystallinity. The assignment of l_1 and l_2 would thus be rather straightforward if the bulk crystallinity is greater than 0.5, because in this case the larger length, l_2, must correspond to the crystal thickness and l_1 to the amorphous layer thickness. Moreover, if l_1 and l_2 at various T_c's are obtained, the assignments may be facilitated by examining the T_c dependences of these two parameters in that the crystal thickness must increase with increasing T_c while the amorphous layer thickness does not necessarily follow this trend.

Because the bulk crystallinities lie above 50% for the majority of blend compositions investigated ($0 \leq w_{PVAc} \leq 0.3$), l_1 and l_2 were assigned as l_a and l_c, respectively. Figure 4a–c plots L, l_c, and l_a against the weight fraction of PVAc (w_{PVAc}). The number-average long period increases with w_{PVAc} over the T_c range investigated. For a given composition, l_c increases with T_c whereas l_a does not, which provides further support for the present assignments of l_1 and l_2. The values of l_c and l_a of neat PHB agree quite well with those reported by Canetti et al.[29] The PHB crystals formed in the blends are thicker than those produced in the pure melt, as l_c is seen to increase with PVAc composition. Formation of thicker crystals in miscible blends has been observed in systems such as PEO/ethylene–methacrylic acid copolymer,[17] PEO/styrene-*p*-hyroxystyrene copolymer,[17] and polycaprolactone/poly(4-vinylphenol).[19] This was attributed to the depression of equilibrium melting point (T_m^0), which lowers the degree of supercooling at a given T_c.[17,19] Depression of T_m^0 in PHB/PVAc has been demonstrated in the prior study.[12] According to the secondary nucleation theory, the initial crystal thickness is given by[30,31]

$$l_g^* = \frac{2\sigma_e T_m^0}{\Delta h_f^0 (T_m^0 - T_c)} + \delta l \tag{5}$$

where σ_e is the fold surface free energy and Δh_f^0 is the bulk enthalpy of melting per unit volume. At low to moderate degree of supercooling, δl is small, eq 5 thus reduces to

$$l_g^* \cong \frac{2\sigma_e T_m^0}{\Delta h_f^0 (T_m^0 - T_c)} \tag{6}$$

The final crystal thickness, according to the notation of Hoffman and Weeks,[30,31] is γ times the initial thickness, i.e.,

$$l_c = \gamma l_g^* \tag{7}$$

where γ is the so-called "lamellar thickening factor". Equation 6 prescribes that the initial crystal thickness is inversely proportional to the degree of supercooling. Because depression of T_m^0 upon blending lowers the degree of supercooling at a given T_c, the larger l_g^* may lead to the formation of thicker crystals in the blends.

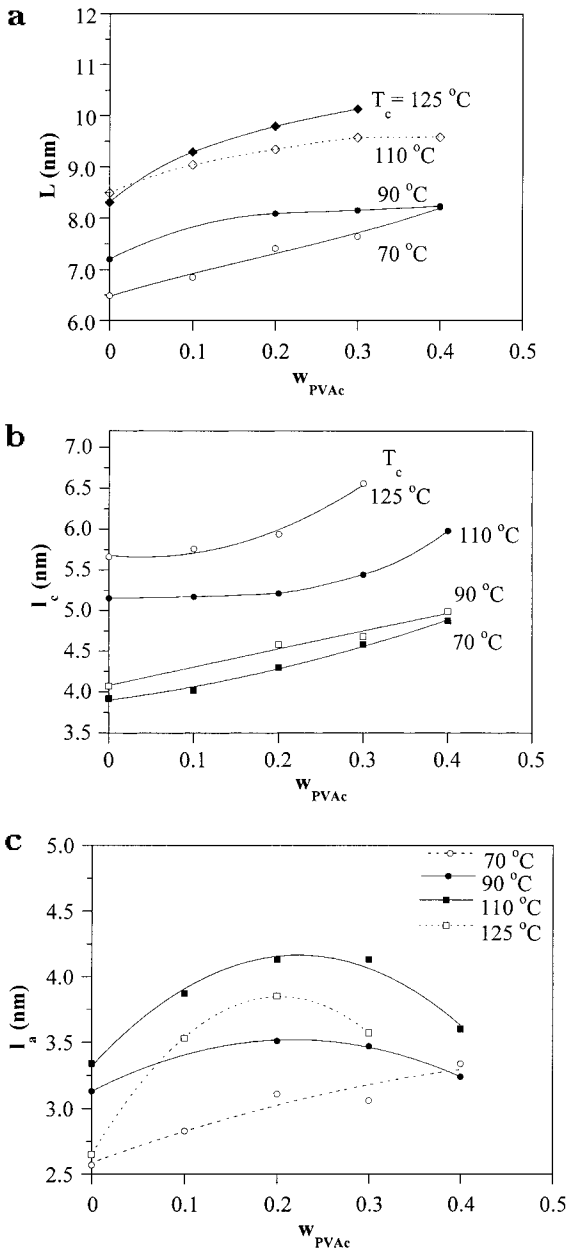

Figure 4. Variations of (a) number-average long period, (b) crystal thickness, and (c) amorphous layer thickness with PVAc composition. The crystallization temperatures are indicated in the figure.

The effect of PVAc composition on the thickness of the amorphous layers is demonstrated in Figure 4c. The blends exhibit larger l_a than neat PHB, meaning that PVAc was incorporated into the interlamellar regions after PHB crystallization. Despite the swelling of the amorphous layers, l_a exhibits a maximum at $w_{PVAc} \approx 0.2$, except for $T_c = 70$ °C where l_a increases monotonically with PVAc composition. In the case of complete interlamellar segregation, l_a must rise monotonically with w_{PVAc}; the presence of a maximum in Figure 4c indicates that a portion of PVAc must have been expelled out of the interlamellar regions as the content of PVAc exceeded 20 wt %, and the extent of extralamellar segregation rises with the increase of PVAc content.

Partial extralamellar segregation at the PVAc composition of 40 and 50 wt % can also be verified by the

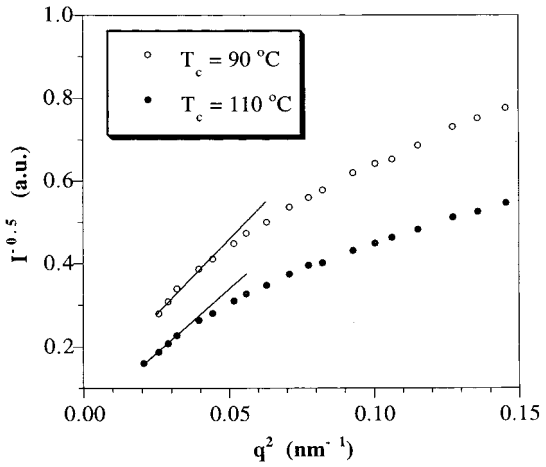

Figure 5. Debye−Bueche plots of 50/50 blend crystallized at 90 and 100 °C. Deviation from the initial linearity occurs at $q \approx 0.2$ nm^{-1} due to the contribution of the scattering associated with the lamellar stacks.

observation of the "zero-angle scattering" in the Lorentz-corrected profiles in Figure 2. For 60/40 blend crystallized at 110 and 125 °C and 50/50 composition crystallized at 90−125 °C, the scattering intensity shows an upturn at the low-q region. Instead of a simple peak, the intensity profiles of these compositions are characterized by the superposition of a monotonically decayed profile and a peak associated with the lamellar stacks. The large low-q intensity or "zero-angle scattering" signifies the presence of a heterogeneity having the size larger than the crystalline and amorphous layers. Such a zero-angle scattering has been observed for PBT/polyarylate,[32] isotactic-PHB/atactic-PHB,[33] and PEO/poly(ethylene succinate)[34] where the morphology was induced by liquid−solid phase separation and for polycaprolactone/polystyrene oligomer[35] and PET/poly(ether imide)[36] where morphology was induced by combined crystallization and liquid−liquid demixing. The size of the heterogeneity associated with the zero-angle scattering has been estimated by the correlation length defined by the Debye−Bueche random structured two-phase model.[34−36] The Debye−Bueche equation reads[37]

$$I(q) = \frac{A}{(1 + a_c^2 q^2)^2} \tag{8}$$

where A is a constant and a_c is the correlation length. Figure 5 shows the Debye−Bueche plots of 50/50 blend crystallized at 90 and 110 °C. Good linearity is observed at the low-q region, while deviation from the initial linearity starts at $q \approx 0.2$ nm^{-1}. Deviation at higher q is due to the contribution of the scattering associated with the lamellar stacks. The Debye−Bueche analysis was not performed for 60/40 blend and 50/50 composition crystallized at 125 °C, because of the strong interference from the scattering peak associated with the lamellar stacks. The average correlation length deduced from Figure 5 is about 9.3 nm. This value is larger than the thickness of the crystalline and amorphous layers, which confirms that the size of the heterogeneity is larger than that of the two types of layers.

According to Schultz,[38] the zero-angle scattering exhibited by semicrystalline polymers may be attributed to the presences of large (greater than lamellar length scales) individual amorphous domains located between

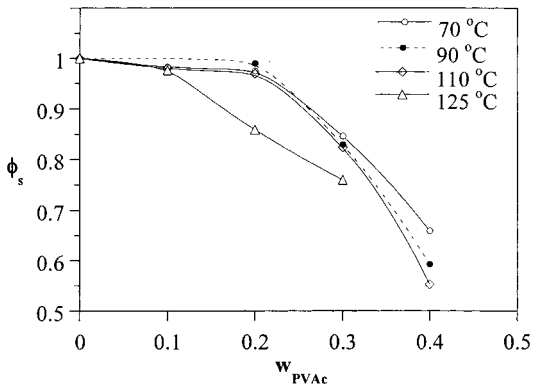

Figure 6. Composition variation of ϕ_s. Except for $T_c = 125$ °C, ϕ_s remains essentially constant at approximately unity when $w_{PVAc} \leq 0.2$. Above this composition, ϕ_s drops obviously with increasing PVAc composition.

the lamellar bundles so as to generate gaps in the sequential stacking of lamellae. In PHB/PVAc blends, these gaps are ascribed to the amorphous domains situated between the lamellar stacks. These amorphous domains were generated by the interfibrillar segregation of PVAc, where PVAc was expelled beyond several layers of lamellae and subsequently resided in the regions between the lamellar stacks.

It should be noted that zero-angle scattering does not necessarily appear in the Lorentz-corrected profiles even if interfibrillar segregation is evident. If the interfibrillar segregation distance is so large (e.g., approaches the order of micrometers) that the amorphous diluent is expelled beyond many layers of lamellae, the interference between the resultant large lamellar stack domains and interfibrillar amorphous domains could generate the zero-angle scattering at the q region that is too small to be accessed by the typical SAXS instrument.

The presence of a maximum in the composition variation of l_a and observation of zero-angle scattering for the higher PVAc composition (50 and/or 40 wt %) suggest that increasing PVAc content tended to raise the extent of interfibrillar segregation. At the lowest T_c of 70 °C, no noticeable zero-angle scattering was identified for all compositions investigated. Increasing T_c lowered the minimum PVAc composition exhibiting the zero-angle scattering, suggesting that interfibrillar segregation was facilitated by raising T_c. The effects of composition and T_c on the extent of interfibrillar segregation can be further evaluated from the magnitude of the volume fraction of lamellar stacks, ϕ_s, which is given by

$$\phi_s = \phi_c / \phi_c^{\,\mathrm{lin}} \tag{9}$$

The magnitude of ϕ_s is closely connected with the morphological structure. In the case of complete interlamellar segregation, the whole sample is homogeneously filled with lamellar stacks, so $\phi_s = 1$. A smaller ϕ_s implies a larger extent of extralamellar segregation. Figure 6 plots ϕ_s as a function of PVAc composition. Except for $T_c = 125$ °C, ϕ_s remains essentially constant at approximately unity when $w_{PVAc} \leq 0.2$, meaning that the morphological structure in this composition range is predominantly characterized by the interlamellar segregation. Above 20 wt % PVAc composition, ϕ_s drops obviously with increasing PVAc composition, indicating that interlamellar and interfibrillar segregation coexist, and the extent of interfibrillar segregation increases

with the increase of PVAc composition. ϕ_s is basically lower at higher T_c (this effect is particularly evident for 60/40 composition), confirming the promotion of extralamellar segregation with increasing T_c.

On the basis of the composition variation of l_a, the presence of zero-angle scattering, and the magnitude of ϕ_s, it is affirmatively established that the segregation distance of PVAc was promoted by increasing PVAc composition and temperature. These effects can be interpreted by the postulate that crystal growth rate is the dominant factor to control the segregation distance of the amorphous diluent.[17−19] Slower growth rate may result in a larger extent of extralamellar segregation, since the amorphous diluent can diffuse out more easily and avoids being trapped inside the interlamellar regions. Because the crystallization kinetics of PHB is dominated by the thermodynamic driving force over the T_c range investigated, the crystal growth rate decreases with increasing T_c. At higher T_c such as 110 and 125 °C, the slower growth rate and better diluent mobility (compared with those at 70 and 90 °C) allow PVAc to be expelled by a larger distance. Similarly, longer segregation distance is induced by increasing PVAc composition because of the stronger depression in crystal growth rate.

Conclusions

The effects of composition and crystallization temperature on the morphological structure of PHB/PVAc blends have been investigated. Blending with PVAc increased the thickness of PHB crystals due to the depression of equilibrium melting point which consequently lowered the degree of supercooling at a given T_c. On the basis of the composition variation of l_a, the observation of zero-angle scattering, and the magnitude of ϕ_s, it was concluded that when PVAc composition was ≤20 wt %, the morphology was predominantly characterized by the interlamellar segregation; above this composition, interlamellar and interfibrillar segregation coexisted, and the extent of interfibrillar segregation increased with the increases of PVAc composition and crystallization temperature. Crystal growth rate was proposed to dominate the segregation distance of PVAc. At higher T_c, the slower growth rate allowed PVAc to diffuse out more easily and avoided being trapped inside the interlamellar regions. Increasing PVAc composition induced a stronger depression in growth rate and consequently promoted the extent of interfibrillar segregation.

Acknowledgment. This work is supported by the National Science Council, R.O.C. under Grant NSC 88-2216-E-007-014 and also in part by the Division of Materials Sciences, U.S. Department of Energy, under Contract DE-AC05-96OR22464 with Lockheed Martin Energy Research, Corp.

References and Notes

(1) Avella, M.; Martuscelli, E. *Polymer* **1988**, *29*, 1731.
(2) Avella, M.; Martuscelli, E.; Greco, P. *Polymer* **1991**, *32*, 1647.
(3) Kumagai, Y.; Doi, Y. *Polym. Degrad. Stab.* **1992**, *35*, 87.
(4) Avella, M.; Martuscelli, E.; Raimo, M. *Polymer* **1993**, *34*, 3234.
(5) Marand, H.; Collins, M. *ACS Polym. Prepr.* **1990**, *31*, 552.
(6) Edie, S. L.; Marand, H. *ACS Polym. Prepr.* **1991**, *32*, 329.
(7) McCarthy, S. P.; Gross, R. *Proceedings of Environmentally Degradable Polymers: Technical, Business, and Public Perspectives*; Chelmsford, MA, 1991.
(8) Dave, B.; Parikh, M.; Reeves, M. S.; Gross, R. A.; McCarthy, S. P. *Polym. Mater. Sci. Eng.* **1990**, *63*, 726.
(9) Dubini Paglica, E.; Beltrame, P. L.; Canetti, M.; Seves, A.; Marcandalli, B.; Martuscelli, E. *Polymer* **1993**, *34*, 996.
(10) Sadocco, P.; Canetti, M.; Seves, A.; Martuscelli, E. *Polymer* **1993**, *34*, 3368.
(11) Iriondo, P.; Iruin, J. J.; Fernandez-Berridi, M. J. *Macromolecules* **1996**, *29*, 5605.
(12) Greco, P.; Martuscelli, E. *Polymer* **1989**, *30*, 1475.
(13) Kumagai, Y.; Doi, Y. *Polym. Degrad. Stab.* **1992**, *36*, 241.
(14) Stein, R. S.; Khambatta, F. B.; Warner, F. P.; Russell, T.; Escala, A.; Balizer, E. *J. Polym. Sci., Polym. Symp.* **1978**, *63*, 313.
(15) Russell, T. P.; Ito, H.; Wignall, G. D. *Macromolecules* **1988**, *21*, 1703.
(16) Defieuw, G.; Groeninckx, G.; Renaers, H. *Polymer* **1989**, *30*, 595.
(17) Talibuddin, S.; Wu, L.; Runt, J. P.; Lin, J. S. *Macromolecules* **1996**, *29*, 7527.
(18) Chen, H.-L.; Li, L.-J.; Lin, T.-L. *Macromolecules* **1998**, *31*, 2255.
(19) Chen, H.-L.; Wang, S.-F.; Lin, T.-L. *Macromolecules* **1998**, *31*, 8924.
(20) Wenig, W.; Karasz, F. E.; MacKnight, W. J. *J. Appl. Phys.* **1975**, *46*, 4194.
(21) Khambatta, F. B.; Warner, F.; Rusell, T. P.; Stein, R. S. *J. Polym. Sci., Polym. Phys. Ed.* **1976**, *14*, 1391.
(22) Russell, T. P.; Stein, R. S. *J. Polym. Sci., Polym. Phys. Ed.* **1983,** *21*, 999.
(23) Barham, P. J.; Keller, A.; Otun, E. L.; Holmes, P. A. *J. Mater. Sci.* **1984**, *19*, 2781.
(24) Santa Cruz, C. S.; Stribeck, N.; Zachmann, H. G.; Balta′ Calleja, F. J. *Macromolecules* **1991**, *24*, 5980.
(25) Stribeck, N.; Alamo, R. G.; Mandelkern, L.; Zachmann, H. G. *Macromolecules* **1991**, *24*, 5980.
(26) Albrecht, T.; Strobl, G. *Macromolecules* **1996**, *29*, 783.
(27) Strobl, G. R.; Schneider, M. *J. Polym. Sci., Polym. Phys. Ed.* **1980**, *18*, 1343.
(28) Cowley, J. M. *Diffraction Physics*, 2nd ed.; North-Holland; Amsterdam, 1981.
(29) Canetti, M.; Urso, M.; Sadocco, P. *Polymer* **1999**, *40*, 2587.
(30) Hoffman, J. D.; Weeks, J. J. *J. Res. Natl. Bur. Stand. A: Phys. Chem.* **1962**, *66A*, 13.
(31) Hoffman, J. D.; Miller, R. L. *Polymer* **1997**, *38*, 3151.
(32) Huo, P. P.; Cebe, P.; Capel, M. *Macromolecules* **1993**, *26*, 4275.
(33) Abe, H.; Doi, Y.; Satkowski, M. M.; Noda, I. *Macromolecules* **1994**, *27*, 50.
(34) Chen, H.-L.; Wang, S.-F. *Polymer*, submitted for publication.
(35) Nojima, S.; Satoh, K.; Ashida, T. *Macromolecules* **1991**, *24*, 942.
(36) Chen, H.-L.; Hsiao, M.-S. *Macromolecules* **1998**, *31*, 6579.
(37) Debye, P.; Bueche, A. M. *J. Appl. Phys.* **1949**, *20*, 518.
(38) Schultz, J. M. *J. Polym. Sci., Polym. Phys. Ed.* **1976,** *14*, 2291.

MA990304+